ARCHITECTURE CIVIL ENGINEERING ENVIRONMENT
The Silesian University of Technology No. 1/2019

doi: 10.21307/ACEE-2019-006

SHEAR BUCKLING RESISTANCE OF CANTILEVER GIRDERS WITH CORRUGATED WEB

Witold BASIŃSKI *

*PhD Eng.; Faculty of Civil Engineering. The Silesian University of Technology, Akademicka 5, 44-100 Gliwice, Poland
E-mail address: *witold.basinski@polsl.pl*

Received: 19.07.2018; Revised: 19.10.2018; Accepted: 24.01.2019

Abstract
The study reports investigations into shear buckling resistance of the corrugated web of cantilever SIN girders. Experimental tests were conducted on ten SIN girders with the web height of 500, 1000, 1250 and 1500 mm made to 1:1 scale. The tests confirmed the advantageous effect of support stiffeners of cantilever girder parts on shear buckling resistance. Load-displacement paths of global displacements in cantilevers of SIN girders were analysed. The Finite Element Method was used to construct models that simulated the behaviour of the experimental models. The numerical analysis of FEM girders was conducted for twelve models with the web height ranging from 500 to 1500 mm, and web thickness of 2, 2.5 and 3 mm. In the FEM analysis, different modes of the web failure, namely local and interactive ones, were taken into account. Based on experimental investigations and the FEM analysis, a method for estimating design shear buckling resistance of the corrugated web in cantilever girders with support stiffener was proposed. The method was based on the determination of interactive buckling resistance. It was demonstrated that support stiffeners in cantilever girders produced an advantageous effect on increase in shear buckling resistance. The solution developed was compared with the methods currently employed to determine buckling resistance. Conclusions and recommendations were drawn on dimensioning of cantilever girders with support stiffener.

Keywords: **Cantilever girders with corrugated web type SIN; Interactive shear buckling resistance; Design shear buckling resistance; Support stiffener; Finite element method.**

1. INTRODUCTION

Welded plate girders with thin-wall corrugated webs, lower in weight than conventional plate girders, have gained in popularity in 90's. Currently, SIN girders available on the market have three basic web thicknesses of 2.0, 2.5 and 3.0 mm and heights ranging from 333 to 1500 mm. Guaranteed by the manufacturer, yield resistance of the corrugated web steel is f_y = 215 MPa.

Due to the web thickness, SIN girders are more stressed in shear compared with flat webs. The buckling mechanism in sinusoidal corrugated web under shear load is still classified separately as a local and global instability [1]. However, for girders with the trapezoidal web used in bridge structures, web failure modes showing the characteristics of local and global instability, are currently classified as the web interactive instability [2, 3, 4, 5, 6, 7]. Investigations into girders with trapezoidal web conducted so far have produced many models for estimating interactive shear buckling resistance [2, 5, 6, 8, 9, 10, 11]. The models are based on the interaction of stress in local and global web instability and shear yield strength. The solutions proposed did not include webs with corrugated folds. In 2009, Eldib [12] put forward a solution for bridge girders with corrugated webs of trapezoidal folds. The equation of the design buckling resistance was based on the regression curve obtained from FEM investigations.

In the author's studies [13, 14], observations were made that in SIN girders, a relation holds between local and global mode of instability in shear. That

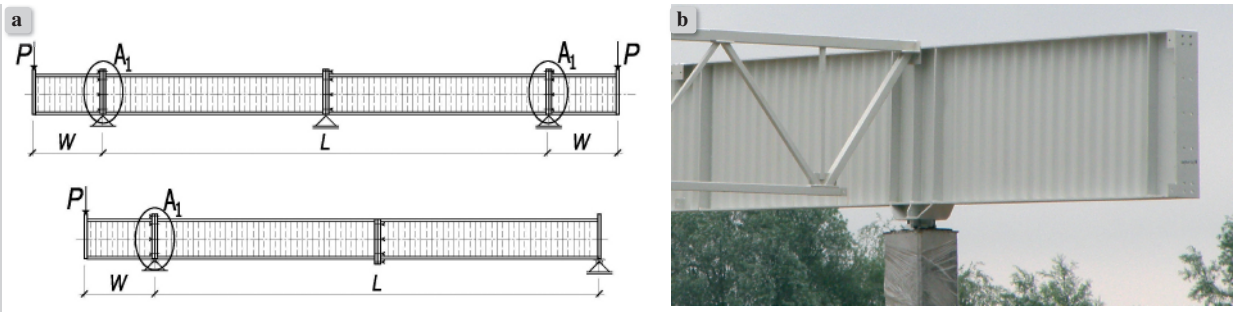

Figure 1.
Cantilever SIN girders: a) static scheme, b) flat plates on the support in the SIN girder

results in the fact that shear buckling resistance of the corrugated web of SIN girders stated in the code [1] is overestimated. In studies [13, 15], it was shown that vertical stiffeners located at the ends of simply supported girders substantially contribute to an increase in shear buckling resistance of the corrugated web. The problem of instability in SIN girders with semi-rigid and rigid support stiffeners was discussed in study [15].

Based on preliminary investigations, it is known that for cantilever girders under two-sided symmetrical load on cantilevers (Fig. 1a), load P on the cantilever does not weaken support parts of the web in the cantilever span. Conversely, for a one-sided cantilever (Fig. 1b), a substantial effect of cantilever load on the girder span is found. In such situations, it is necessary to account for cantilever load influence on the web shear stress in the span. Additionally, it is common to use flat transition sheet in beam joints at support stiffeners [16].

This study reports investigations into shear buckling resistance of the corrugated web of SIN girders with one-sided cantilever (Fig. 1b). The advantageous effect of support stiffeners, denoted as A_1 in Fig. 1, was confirmed. The beneficial effect also included shear buckling resistance of girders. Furthermore, it was checked whether it is necessary to use additional flat transition sheet at beam-to-stiffener joints, which is recommended in the Guidelines [16].

Experimental investigations on end-loaded one-sided cantilever were conducted using ten girders with the web height of 500, 1000, 1250 and 1500 mm, composed of three pre-assembled units. Girders, the loading diagram of which corresponded to a simply supported beam with one-sided cantilever, were constructed from pre-assembled units, butt-connected using HV bolts.

The Finite Element Method was used to simulate experimental investigations [17]. The FEM analysis was applied to numerically estimate design buckling resistance of the corrugated web of cantilever girders. The FEM numerical analysis of buckling resistance of cantilever girders was carried out using models with the web height ranging from $h_w = 500$ to $h_w = 1500$, and web thickness of 2.0, 2.5 and 3 mm. The method for estimating design shear buckling resistance of the corrugated web of cantilever girders with support stiffener was shown. The method, which is consistent with the experimental results for cantilever girders, is based on the determination of interactive buckling resistance.

2. DESIGN SHEAR BUCKLING RESISTANCE OF GIRDERS WITH CORUGATED WEB

For girders with trapezoidal profile of the web folds, the estimation of design shear buckling resistance was based on the computation of the interactive buckling resistance. The general form of the equation describing interactive buckling resistance τ_{crI} is given by the following formula:

$$\left(\frac{1}{\tau_{crI}}\right)^n = \left(\frac{1}{\tau_{crL}}\right)^n + \left(\frac{1}{\tau_{crG}}\right)^n, \qquad (1)$$

where: $n = 1$ [2], $n = 2$ [8], $n = 4$ [11].

Equation (1) relates stresses at the web local τ_{crL} and global τ_{crG} instability. Some researchers additionally supplemented solution (1) by including the effect produced by shear yield strength τ_y. That can be found in studies [5] and [9].

In 2009, Moon [18] proposed a solution (4) that was based on interactive buckling resistance Y_i [7]. In Moon's solution, in order to determine design buckling resistance, it is necessary to estimate slenderness λ_s (2), which depends on interactive buckling parameter k_I (3). In the adopted solution, design buckling

resistance was limited to the value of shear yield strength τ_y.

$$\lambda_s = 1.05\sqrt{\frac{\tau_y}{k_I E}}\left(\frac{h_w}{t_w}\right), \tag{2}$$

$$k_I = \frac{30.54}{5.34\left(h_r/t_w\right)^{-1.5} + 5.72\left(w/h_w\right)^{-1.5}}, \tag{3}$$

$$\frac{\tau_{n,M}}{\tau_y} = \begin{cases} 1.0 & for \quad \lambda_s \le 0.6 \\ 1 - 0.614\left(\lambda_s - 0.6\right) & for \quad 0.6 < \lambda_s \le \sqrt{2} \\ 1/\lambda_s^2 & for \quad \sqrt{2} < \lambda_s \end{cases} \tag{4}$$

In 2011, Sause and Braxtan presented their solution [6] expressed in the form of equation (5), in which design buckling resistance was dependent on interactive slenderness computed acc. formula (6).

$$\tau_{n,SB} = \tau_y\left(\frac{1}{\lambda_{I,3}{}^6 + 2}\right)^{1/3}, \tag{5}$$

$$\lambda_{I,3} = \lambda_L\lambda_G\left(\left(\frac{1}{\lambda_L}\right)^6 + \left(\frac{1}{\lambda_G}\right)^{2n}\right)^{1/6} \tag{6}$$

$$\lambda_L = \sqrt{\frac{12\left(1-\nu^2\right)\tau_y}{k_L\pi^2 E}}\,\frac{w}{t_w} \tag{7}$$

$$\lambda_G = \sqrt{\frac{12h_w^2\tau_y}{k_G F(\alpha,\beta) E t_w^{0.5} b^{1.5}}} \tag{8}$$

In the solution of concern, local and global slenderness was determined from formula (7) and (8). Additionally, the factor for global instability k_G, ranging from 36 to 68.4, was based on Easley's concept [19]. Moreover, coefficient $F(\alpha, \beta)$ was determined from equation (9) [2].

$$F(\alpha,\beta) = \sqrt{\frac{(1+\beta)sin^3\alpha}{\beta + cos\,\alpha}}\cdot\left(\frac{3\beta+1}{\beta^2(\beta+1)}\right)^{0.75} \tag{9}$$

where β is the ratio of the sides of the trapezoidal folds (b/c) and α is the inclination angle of folds.

All available solutions concerning the computation of design shear buckling resistance relate to webs with trapezoidal shape of folds. In 2009, Eldib [12] put forward a solution for wave-shaped webs. The shape corresponded to the trapeze geometry used in bridge girders. The solution was based on regression analysis obtained from FEM investigations.

As regards SIN girders utilizing sine-shaped folds, the solution currently used can be found in EC3 [1]. In this solution, it is necessary to calculate stresses separately at local τ_{crL} and global τ_{crG} instability. As a result, Equation (10) describing shear buckling stress at local instability, based on the classical buckling theory for flat sheet, has the following form:

$$\tau_{crL} = \left(5.34 + \frac{a_w \cdot s}{h_w t_w}\right)\frac{\pi^2 E}{12\left(1-\upsilon^2\right)}\left[\frac{t_w}{s}\right]^2, \tag{10}$$

where $E = 210$ GPa – modulus of elasticity, v – Poisson's ratio; $s = 89$ mm – length of the arc of half-sine wave; $a_w = 40$ mm – height of the two half-sine waves, h_w, t_w – web height and thickness.

Next, the dependence describing shear buckling stress at global instability based on the stiffness relation of the orthotropic plate [19], a replacement for the corrugated web, can be expressed by equation:

$$\tau_{crG} = 32.4\frac{\left(D_y D_z^3\right)^{1/4}}{t_w h_w^2}, \tag{11}$$

where: D_y – orthotropic plate bending stiffness in a plane perpendicular to generatrix of the web shell;

D_z – orthotropic plate bending stiffness in a plane parallel to generatrix of the web shell.

The solution offered by EC3 [1] does not account for the interaction between local and global shear instability. The formula for estimating design shear resistance acc. [15] based on the determination of interactive buckling resistance was approximated for cantilever girders. It is presented in Chapter 6.

3. EXPERIMENTAL INVESTIGATIONS

In order to determine shear buckling resistance of cantilever girders with support stiffeners, experimental investigations were conducted. They covered ten SIN girders with a loading diagram that corresponded to a simply supported beam with one-sided cantilever. (Fig. 2). All corrugated web girders were designed and fabricated compliant with the literature and standards [1, 16].

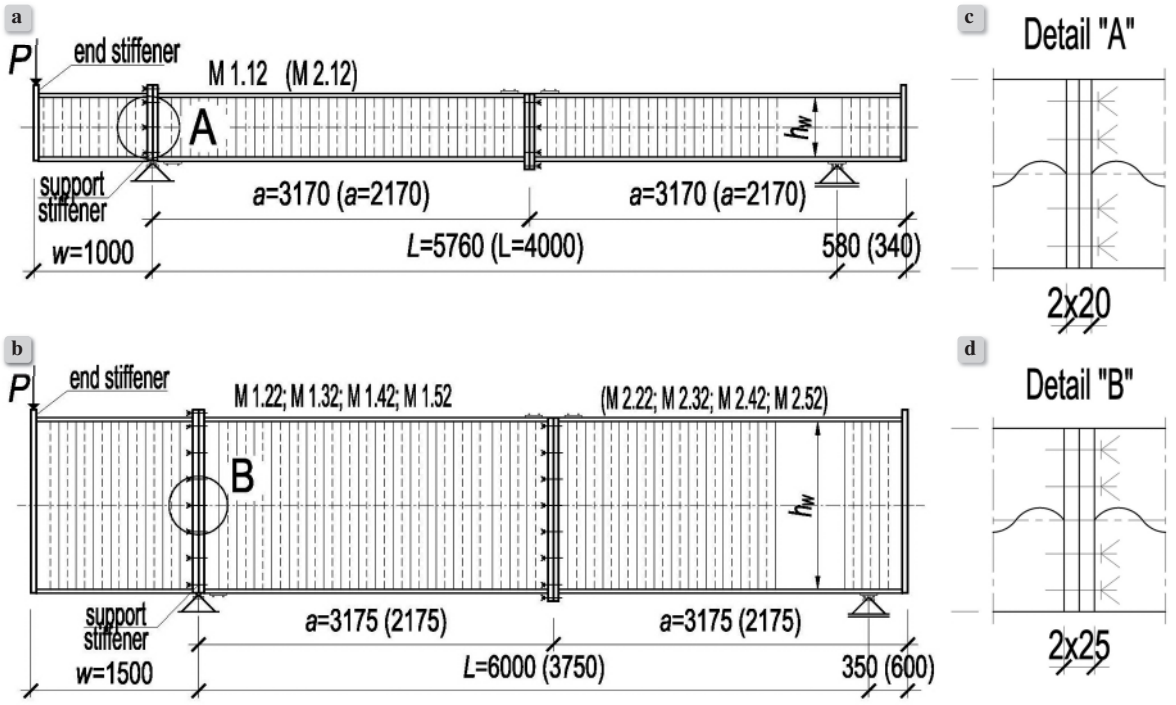

Figure 2.
Cantilever girders with corrugated web a) models M 1.12, M 2.12 b) models M 1.22, M 1.32, M 1.42, M 1.52, M 2.22, M 2.32, M 2.42, M 2.52; c) d) end stiffeners

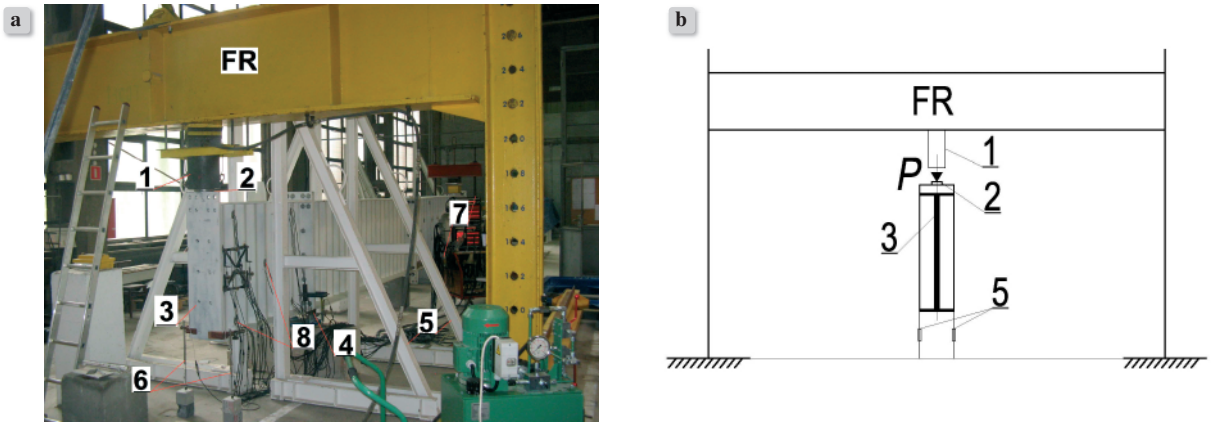

Figure 3.
a) Girder 2.32 on the test stand; b) steel frame FR

Girders were made from pre-fabricated pre-assembled units. Girders with the web height of h_w = 500 mm (Fig. 2a) consisted of a cantilever part, w = 1.0 m in length, and span parts that were a = 3.17 m and a = 2.17 m long. Girders with the web heights of h_w = 1000, 1250 and 1500 mm (Fig. 2b) were composed of a cantilever part that had the length of w = 1.5 m, and span parts, the length of which was a = 3.175 m or a = 2.175 m.

In WTA 500 girders (the first two letters WT mean the girder with corrugated web, the next letter means the thickness of the web, that is: A – 2 mm, B – 2.5 mm, C – 3 mm), 20 mm thick end plates were used (Fig. 2a, 2c). In the other girders, end plates 25 mm in thickness were employed (Fig. 2b, 2d).

The pre-assembled units of the girders of concern were butt-connected using HV M20 (h_w = 500 mm) and M 24 (h_w = 1000, 1250 and 1500 mm) bolts, class 10.9, the bearing capacity of which was greater than that of girders. The connections satisfied the require-

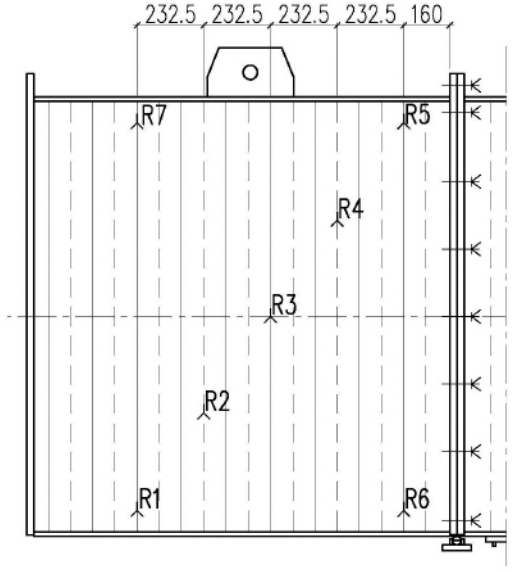

Figure 4.
Location of strain gauges on the girder web M 2.52

ments, from which it follows that rotation in the connection can be treated as a linear function of the rotational stiffness S_j [20, 21]. Girder webs were fabricated, in accordance with the manufacturer's data, of S235JRG2 steel grade, whereas flanges were made from S275 steel grade.

The girders were constructed from pre-assembled units. Openings in the connection end plates were adjusted at the experimental stand, which limited the occurrence of imperfections in end-plate connections. A frame (FR) (Fig. 3b) was constructed to load the girders. The load, in the form of a concentrated force P, was transferred from the frame (FR) by means of the actuator (1) to the pad (2), and then to the end plate of the cantilever part of the girder (3). On the pin support, dynamometers (4) were installed to measure reaction V resulting from the applied load. The cantilever and span parts of girders were secured against lateral torsional buckling (LTB) by additional side supports (5).

The following quantities were measured in the investigations: reaction V (Fig. 3) to load P with the use of dynamometers (4), total displacements y of the girder cantilever part – with a pair of induction sensors (6), girder vertical displacements, pull-off of the end support (7) and corrugated web strain – with an array of strain gauges (8). Strain gauge rosette arrangement for the web strain measurement in an exemplary girder is shown in Fig 4. Load P on girders was increased uniformly in 2 kN increments, until the occurrence of the non-linear displacements of the support. Then, the loading step was reduced to 1 kN. The loading rate was up to 20 kN/min.

3.1. Load – displacements paths $P(y)$ of experimental girders

In order to establish the point of the corrugated web instability, the profiles of strains were determined for all strain gauges glued onto the web. Based on the analysis of graphs for diagonal strain gauges, the onset of instability of the corrugated web was specified. The first buckling load P_{eB} was assumed to occur at the point at which strain-load relationship lost its linear character. It should be emphasised that in all girders the instability onset occurred when the strain did not exceed 1.1‰. Figure 5 illustrates exemplary strain dependence on load for M 1.51 and M 2. 51 girders.

Based on the global displacement y measured at the

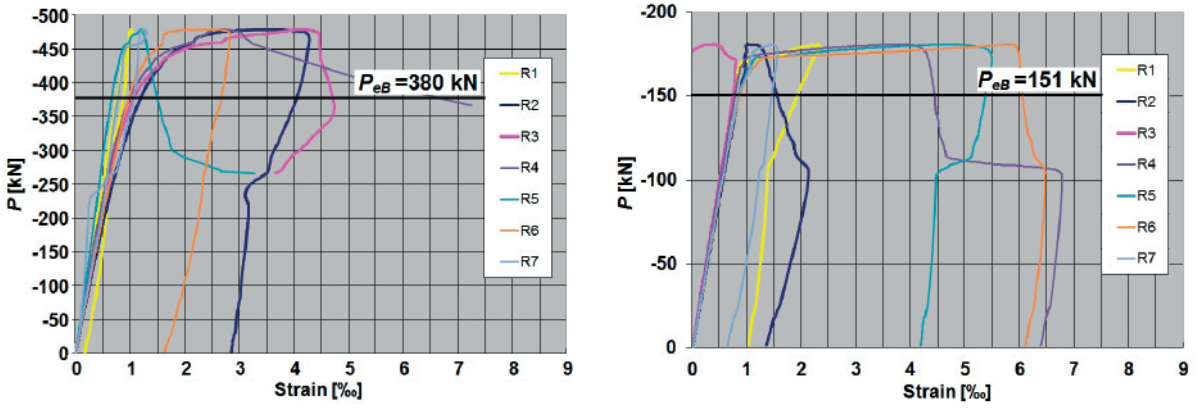

Figure 5.
Strain in the direction 60° relative to the axis of the web a) girder M 1.32; b) girder M 2.12

Table 1.
Experimental results of girders

Girder	Web $h_w \times t_w$ [mm]	Flange [mm]	Suport stiffener	Failure modes	Limit load $P_{u,Rd}$ [kN]	First buckling load P_{eB} [kN]	$P_{eB}/P_{u,Rd}$ [%]
2	3	4	5	6	7	8	9
M 1.12	500x2	300x15	2x300x20	L	184	147	0.80
M 2.12	500x2	300x15	2x300x25	L	181	151	0.82
M 1.22	1000x2	300x20	2x300x25	I	342	298	0.87
M 2.22	1000x2	300x15	2x300x25	L	343	296	0.86
M 1.32	1000x2.6	300x20	2x300x25	I	478	380	0.79
M 2.32	1000x2.6	300x15	2x300x25	I	492	390	0.79
M 2.42	1000x3	300x15	2x300x25	I	694	510	0.73
M 1.42	1250x2	300x15	2x300x25	I	348	304	0.87
M 1.52	1500x2	300x15	2x300x25	I	468	400	0.85
M 2.52	1500x2	300x15	2x300x25	I	459	399	0.87

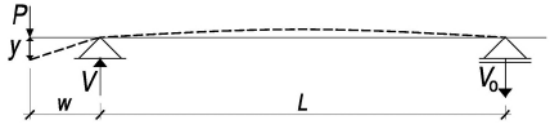

Figure 6.
Diagram of global displacements y of tested girders

end of the girder support (Fig. 6), load-displacement paths LDPs $P(y)$ were determined for all girders.

Figures 7 and 8 show exemplary LDPs $P(y)$ for: M 1.12 and M 2.12 girders with 2×300×20 support stiffener, and also M 1.52 and M 2.52 ones with 2×300×25 support stiffener.

The upper boundary of the rectilinear part of global displacement (point $P_1(P_{eB})$) shown in Figs. 7 and 8 corresponded to the point of instability specified on the basis of strain graph analysis.

Characteristic co-ordinates $P_1(P_{eB})$, $P_2(P_{uRd})$ marked in LDPs $P(y)$ of girders (Figs. 7 and 8) refer to:

$P_1(P_{eB})$ – buckling load of girder, corresponding to the first buckling load P_{eB}. Onset of the web instability;

$P_2(P_{uRd})$ – limit load obtained from the girder limit condition P_{uRd}, related to the failure of the corrugated web;

$P_3(y_3)$ – girder unloading.

The boundary of the range of displacements resulting from the effect of bending moments and shear forces was marked in the global LDPs $P(y)$ as $P_1(P_{eB})$. Point $P_1(P_{eB})$ denotes massive impact exerted by elastic – plastic shear displacements, which leads to the creation of diagonal yield zones in the corrugated web. That results in a considerable increment of shear displacements of supports. Girder supports reach limit load at point $P_2(P_{uRd})$, which closes the range of elastic-plastic strains $P_1(P_{eB}) – P_2(P_{uRd})$.

In cantilever girder with corrugated web, in which support stiffener made from two connected sheets is applied, a large range of elastic strains $0 – P_1(P_{eB})$ is found. The profile of load-displacement paths of cantilever girders with support stiffener shows similarity to the behaviour of simply supported girders with rigid end support stiffeners [15].

Table 1 summarizes the results of experimental investigations into girders. Column 7 shows limit load P_{uRd} measured with force P, whereas column 8 lists first buckling load P_{eB} measured with force P.

3.2. Failrue modes of experimental girders

Failure of the examined girders occurred in the cantilever part, in the area affected by a load induced by a constant shear force. The failure took place suddenly.

The process of the corrugated web instability started from local instability of the sinusoidal panel. In the first stage of girder failure, plastic strains occurred in the corrugated web, adjacent to the tension flange, which led to formation of the web yield zone (1). The latter took the form of diagonal tension line (local instability – L) (Fig. 9a). In girders with the web height starting at $h_w = 1000$ mm, the web instability began with local stability failure near the tension flange. Then the phenomenon evolved to achieve global mode, which resulted in the formation of yield

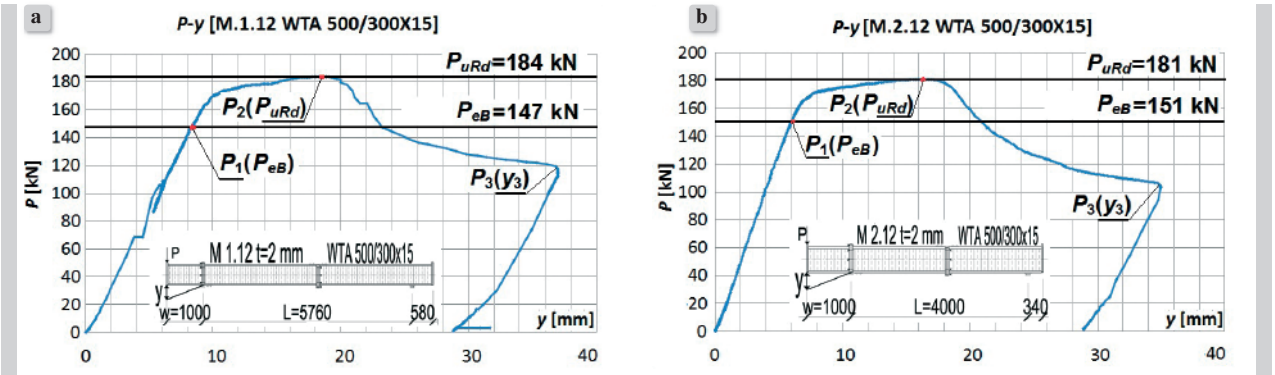

Figure 7.
Load – displacements paths *P*(*y*) of girders a) M 1.12 (2x300x20); b) M 2. 12 (2x300x20 mm)

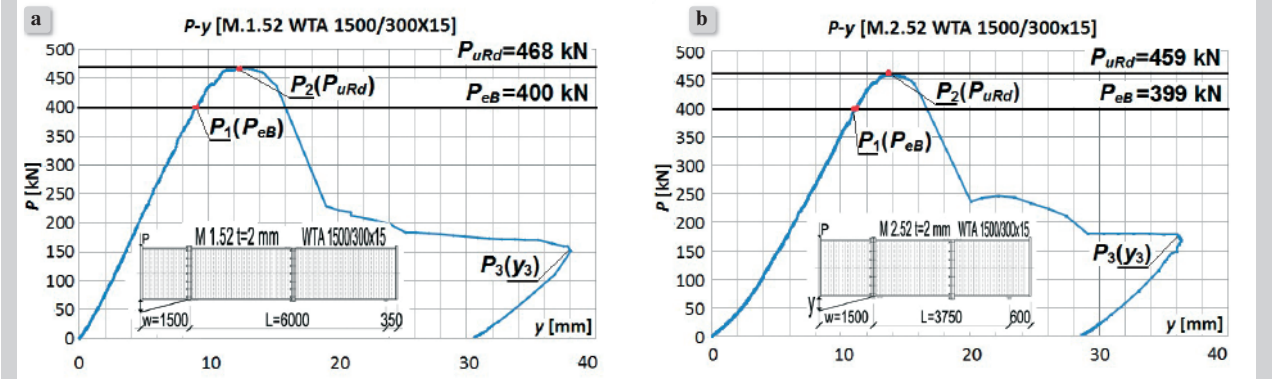

Figure 8.
Load – displacements paths *P*(*y*) of girders a) M 1 .52 (2x300x25 mm); b) M 2. 52 (2x300x25 mm)

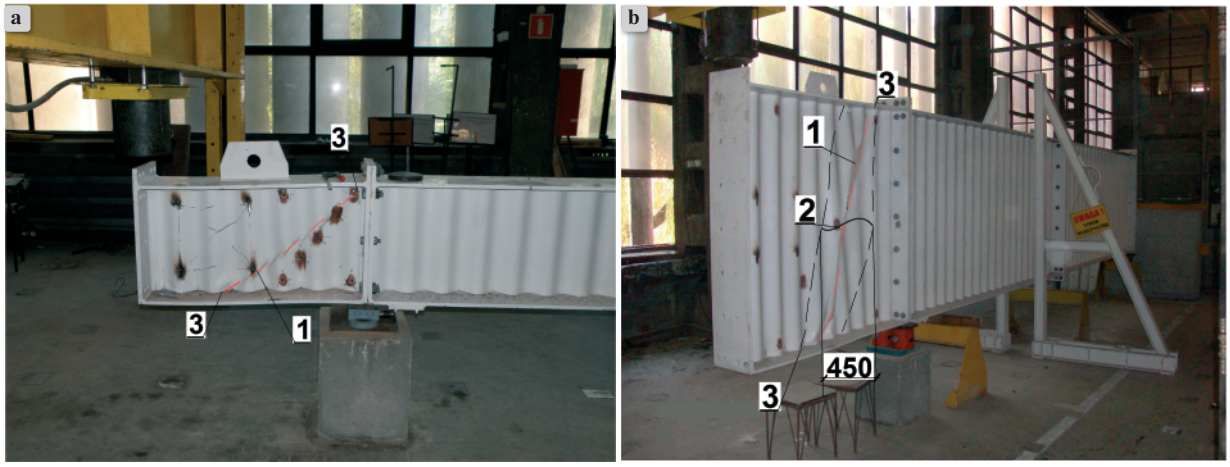

Figure 9.
Failure modes of cantilever SIN girders: a) M 1 .12 (2x300x20 mm); b) M 2. 52 (2x300x25 mm)

zone (1) lines and the snap-through of the adjacent waves of the web (2). As the global mode of instability is triggered by the local one which indirectly affects the web buckling magnitude, it is justified to term the instability interactive (Fig. 9b). In all cantilever girders, at the final stage of failure, tension field together with resistance utilisation in flanges caused the curving of yield zone lines in the direction tangential to flanges and bending (3) of the support flanges in the girder plane.

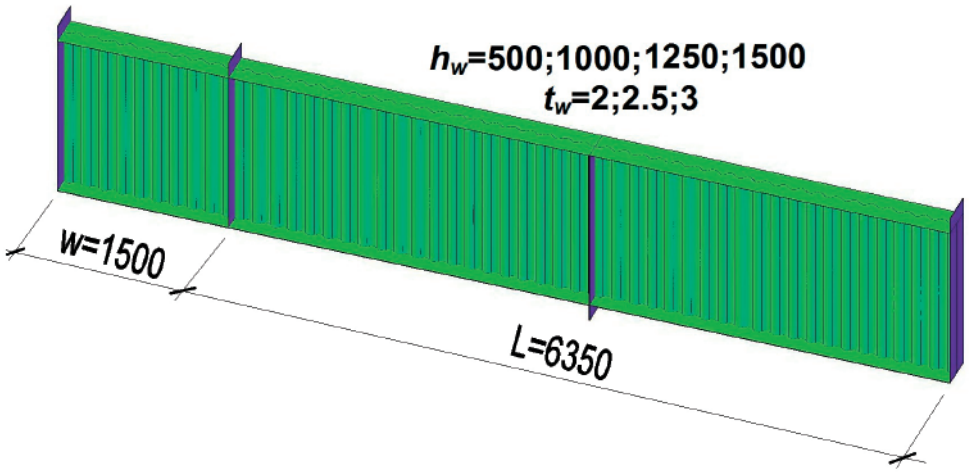

Figure 10.
Numerical models

Table 2.
Current numerical program

h_w [mm]	t_w [mm]	Flange [mm]	Suport stiffener [mm]	w [mm]	L [mm]	Number of models
1	2	3	4	5	7	8
500	2; 2.6; 3	300x15	2x300x20	1500	6350	3
1000	2; 2.6; 3	300x15	2x300x25	1500	6350	3
1250	2; 2.6; 3	300x15	2x300x25	1500	6350	3
1500	2; 2.6; 3	300x15	2x300x25	1500	6350	3

In all tested girders, support stiffener stayed straight and did not bend after the yield zone was formed. The end plate that makes the edging of the stiffeners and end – plate connections of the middle segment also remained intact in all girders.

The above indicates that support stiffener in cantilever girders restricted the action of the tension field and the resulting change in the interaction of compression and shear components along the generatrix of the web. That led to a narrowing of the range of plastic strains $P_1(P_{eB}) - P_2(P_{uRd})$ in cantilever girders, and consequently increased **shear buckling resistance of the corrugated web**.

4. NUMERICAL TESTS

As regards cantilever girders shown in Fig. 10, shear buckling resistance was also estimated numerically. In SIN girders, the dimensions of the web, support stiffeners and flanges interact to affect the failure mode of the corrugated web. Consequently, it was necessary to measure the web height, thickness and wave shape. Also, the dimensions of support stiffeners of flanges were checked. As in the fabrication of SIN girders, the sinusoidal web shape is ensured by the rolling control program, the actual web shape is that of the sine curve. The automation in sheet metal cutting and web welding to flanges and stiffeners in the manufacture of girders additionally limits the occurrence of geometric imperfections in the cross and longitudinal sections of SIN girders. The girders delivered for tests showed only minimal differences in the web thickness. That referred to the web with the nominal thickness of 2.5 mm, the actual thickness of which was 2.6 mm. As regards other experimental girders, their webs were 2 mm and 3 mm thick. Because imperfections of the girder sections may affect failure mode in the corrugated web, measurements of rectilinearity along girders and flange curvature were taken. Experimental girders did not show geometric imperfections either in longitudinal or cross sections. In the numerical models, the geometry of tested girders was simulated based on the experimental investigations. However, as all end – plate connections in experimental girders satisfied the condition that the rotation in the connection could be treated as a linear function of rotational stiffness, they were substituted with intermediate stiffeners.

Table 3.
Material properties

Girder	$\bar{f}_y$ [MPa]	$\bar{f}_u$ [MPa]	Percentage total elongation at maximum force (F_m) [%]	Percentage total elongation at fracture [%]	$\bar{f}_y$ [MPa]	$\bar{f}_u$ [MPa]	Percentage total elongation at maximum force (F_m) [%]	Percentage total elongation at fracture [%]	E [GPa]
	web				flange				
1	2	3	4	5	6	7	8	9	10
M 1.12	334.7	430.6	16.1	22.1	297.5	443.1	23.9	30.3	196
M 2.12	337.9	429.1	15.7	20.8	311.2	476.7	24.5	30.8	188
M 1.22	339.4	435.4	15.9	22.2	287.2	448	24.1	31.4	200
M 2.22	336.3	427.3	14.9	22.5	323.5	461.4	23.1	29.6	234
M 1.32	312.5	453.9	13.8	20.2	264.2	460.9	22.6	28.0	199
M 2.32	324.6	451.5	13.6	19.2	293.9	442.1	25.1	32.3	241
M 2.42	445.9	544.1	10.7	14.6	301.5	439.8	21.3	27.7	205
M 1.42	267.2	360.9	13.4	19.9	302.8	440.4	22.9	30.8	199
M 1.52	299.1	380.5	16.8	23.3	312.5	445.6	24.1	30.0	200
M 2.52	281.0	375.5	17.2	24.6	306.7	449.3	21.9	28.6	203

Their thickness corresponded to that of connection sheets, i.e. 50 or 40 mm (in models with $h_w = 500$ mm). In order to eliminate the impact of the girder lateral torsional buckling (LTB) on the failure mode of the girder web, girders were secured against LTB. Geometric imperfection was represented by the reduction in the web dimension by 1/20 of its thickness acc. [22]

The FEM analysis was conducted using 12 numerical models. All supports were modelled to have the length of $w = 1500$ mm, whereas the length of the span parts was $L = 6350$ mm. The webs of numerical models of 500, 1000, 1250 and 1500 girders were 2, 2.6 and 3 mm in thickness (Fig. 8) (Table 2). The corrugated web was modelled in the CAD environment as a sine curve. The next step involved transferring the curve to the Abaqus program, where the web shape with the pre-set height and length was generated. The flanges, stiffeners and the web were modelled using S4R shell elements (a 4-node doubly curved shell with reduced integration, which has six degrees of freedom at each node, three translations and three rotations) and S3 ones. Altogether, the number of finite elements ranged from 36488 (model $h_w = 500$ mm) to 96417 (model $h_w = 1500$ mm $L = 7825$).

4.1. Materials testing of the steel used in experimental girders

Materials tests on steel in the experimental cantilever girders were conducted using samples cut out of flanges and the web acc. EN [23]. The yield strength of girders was examined on six samples randomly collected from along the web fold of each girder (yield strength variation coefficient ranged from 0.001 to 0.003). As regards flanges, yield strength was examined using three randomly chosen samples. Selected results of the materials tests are shown in Table 3.

In the materials tests conducted on girders, a very **large scatter of the web yield strength results** was found [24]. For the sake of standardization, the materials parameters adopted for all 12 numerical models, were the results obtained for the M 2.52 girder (Table 3). The materials parameters employed in the numerical analysis approximate the yield strength of M 1.42, M 1.52 girders, and also of beam girders analysed in study [15]. That allows making a direct comparison of girders with the numerical analysis results. In numerical investigations, the material model obtained from materials tests of properties of steel utilised in experimental investigations was adopted. The material model accounted for the Huber-Mises-Hencky yield criterion.

4.2. Type of analysis, load and boundary conditions

In all numerical models (Fig. 11), the adopted boundary conditions were the same as for experimental girders (Fig. 2). Numerical models were pin-supported on one side. On the other side, roller support was used on the external end stiffeners. As regards the support beneath the cantilever part, the possibility of vertical ($U_z = 0$), longitudinal ($U_x = 0$) and lateral ($U_y = 0$) displacements was excluded. On the end support, the possibility of vertical ($U_z = 0$) and later-

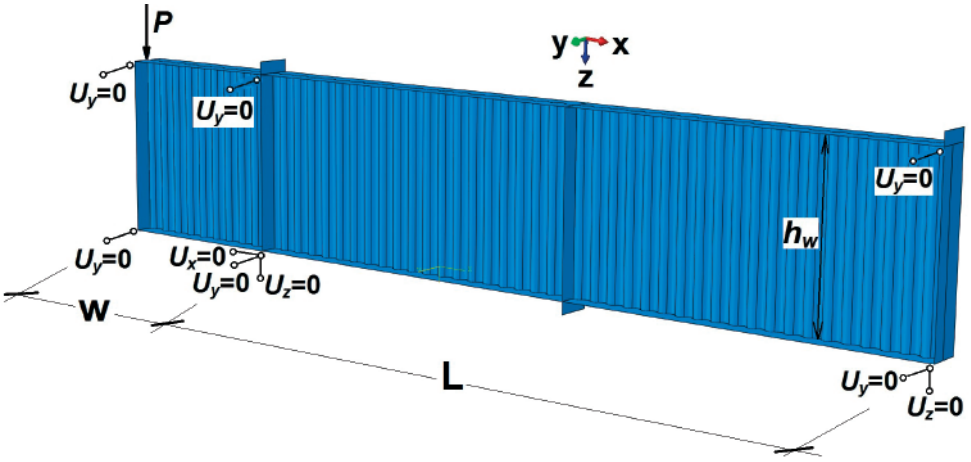

Figure 11.
Boundary conditions and load application to numerical model

Table 4.
Numerical results of girders

Girder h_w x t_w [mm]	Support Stiffener	Failure modes	Limit load $P_{u,Rd}$ [kN]	First buckling load P_{eB} [kN]	$P_{eB}/P_{u,Rd}$ [%]
1	2	3	4	5	6
500x2	2x300x20	L	154.1	149.1	0.97
500x2.5	2x300x20	L	192.2	186.8	0.97
500x3	2x300x20	L	231.3	224.6	0.97
1000x2	2x300x25	L	308.1	297.2	0.96
1000x2.5	2x300x25	I	384.3	371.3	0.97
1000x3	2x300x25	I	462.2	445.3	0.96
1250x2	2x300x25	I	384.6	360.1	0.94
1250x2.5	2x300x25	I	480.4	449.9	0.94
1250x3	2x300x25	I	576.5	539.5	0.94
1500x2	2x300x25	I	460.8	419.2	0.91
1500x2.5	2x300x25	I	575.6	531.9	0.92
1500x3	2x300x25	I	687.5	635.7	0.92

al (U_y=0) displacements was eliminated. To secure cantilever girders against LTB, at the sites of stiffeners, the possibility of horizontal displacements (U_y=0) and girder rotation around axis x (ϕ_x=0) was averted.

Support conditions adopted in numerical investigations represent those used in actual structures. That caused slight extension of the cantilever part in numerical models. However, it did not affect the values of the limit load, buckling load, or shear buckling resistance. Conversely, in experimental girders support conditions included a roller bearing support, and also hinge support. The latter also supported the end of the girder.

The load (Fig. 11) having the form of a concentrated force P was applied to the stiffener that closed the supports. Initially, the loading step was linear. After girder instability occurrence, it became non-linear. Then when limit load was reached, the model was unloaded.

In the numerical analysis reported in this study, the Riks method was used. In this method, the load is proportionally applied in individual steps. The control parameter is the so-called path parameter. The Riks method allows finding a solution to a task regardless of the web failure mode. That is related to identifying load-displacement equilibrium at the end of each iteration step. While seeking load-displacement equilibrium, the load can be increased or decreased until the limit load is reached acc. [25]. The Riks method is very often used in static load analysis as it provides one of the most suitable tools for nonlinear analysis.

4.3. Load – displacements paths $P(y)$ of numerical models

The numerical model was validated in two stages. The first stage of the model validation involved the use of a "perfect model", in which no imperfections occurred, and the geometry of webs, flanges and stiffeners from measurements was accurately represented. For M 2.52 (1500x2) and M 1.42 (1250x2) girders, the ratio of first buckling load P_{eBINV}/P_{eBFE} (first buckling load from test/ first buckling load from FEM analysis) was found to range 11–24%.

In the second stage of the model validation, an "imperfect model" was considered. The imperfection

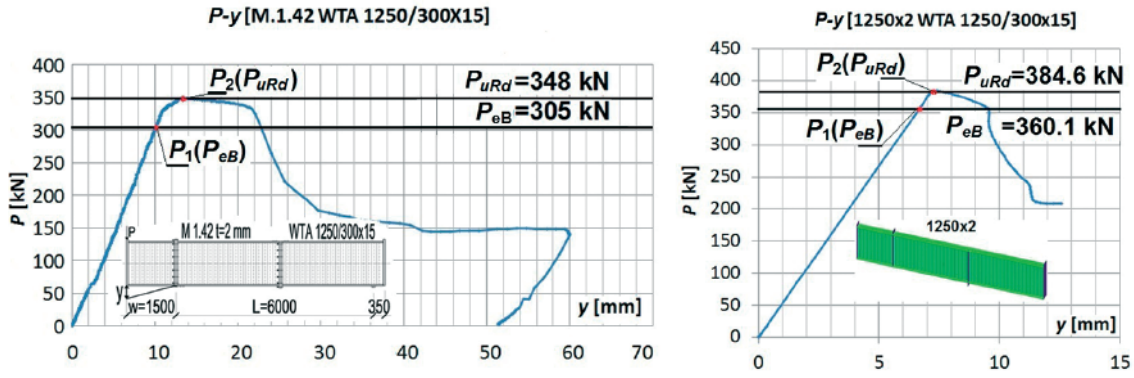

Figure 12.
Comparison of LDPs *P*(*y*): a) tests M 1.42; b) FEM 1250x2

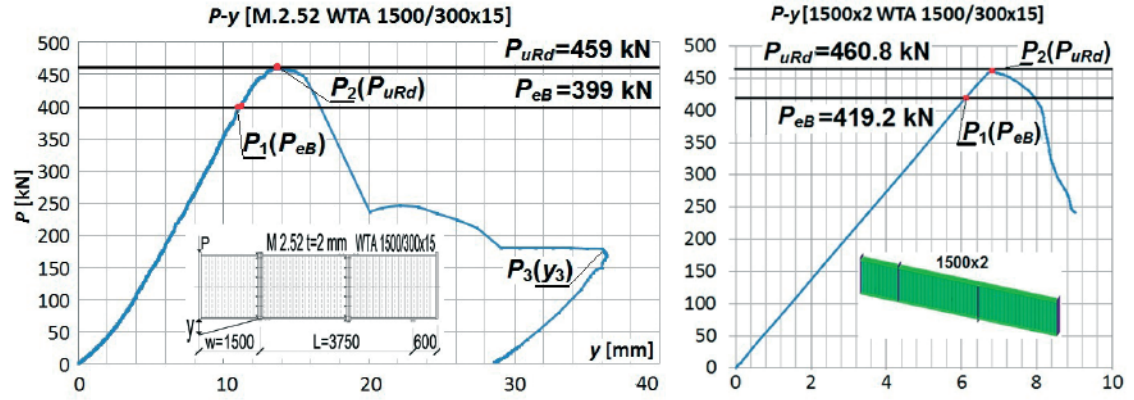

Figure 13.
Comparison of LDPs *P*(*y*): a) test M 2.52; b) FEM 1500x2

consisted in the web thinning by 1/20 of its thickness acc. [22]. Based on the direct comparison of experimental results and the numerical analysis on the example of M 2.52 (1500x2) girder and 1500x2 "imperfect model", it can be stated that the results of estimating the limit load P_{uRd} obtained through the FEM analysis turned out to be congruent with the results of experimental investigations (cf. Table 2 and Table 4). However, when estimating first buckling load P_{eB}, FEM analysis results proved to be 5% higher than experimental results (M 2.52/1500x2). Other validation procedures concerned the comparison of failure modes in numerical and experimental models, and also that of load – displacements paths. In all subsequent numerical models, an initial imperfection, related to a decrease in the web thickness, was assumed. As a result of validation, a satisfactory convergence of results was obtained.

In all remaining numerical models, because of lower yield strength than that in experimental girders, the results of first buckling load turned out to be slightly smaller. The effect of variable yield strength on the results of the design buckling resistance was accounted for in the theoretical solution adopted (Chapters 5 and 6).

Load-displacement paths LDPs $P(y)$ of the global displacement of the support end were determined for all actual and numerical models of girders on the basis of the measured displacement y of the support end.

Figures 12b and 13b show exemplary LDPs $P(y)$ of numerical models of cantilever girders 1250x2 and 1500x2. For the sake of comparison, Figs 12a and 13a illustrate LDPs $P(y)$ obtained on the basis of experimental investigations into M 1.42 (1250x2) and M 2.52 (1500x2) girders. In both cases, profiles of load-displacement paths are very much similar.

In load-displacement paths, characteristic coordinates $P_1(P_{eB})$, $P_2(P_{uRd})$ were marked. They correspond to characteristic points found in experimental investigations.

For each numerical model of cantilever girders, the web instability took place at point $P_1(P_{eB})$, which was related to the occurrence of nonlinearity in LDP $P(y)$

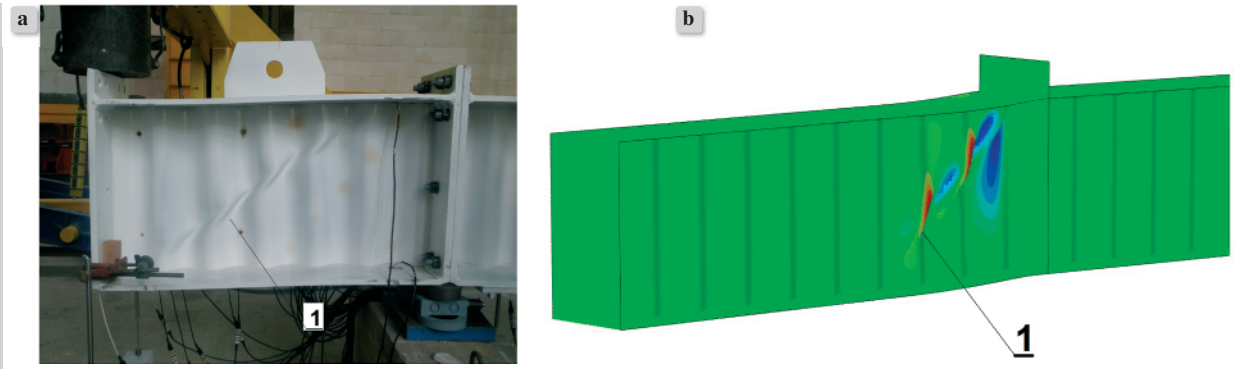

Figure 14.
Comparison of failure modes: a) experimental girder M 1.12 (500x2: stiffener 2x300x20); b) numerical model 500x2 (stiffener: 2x300x20)

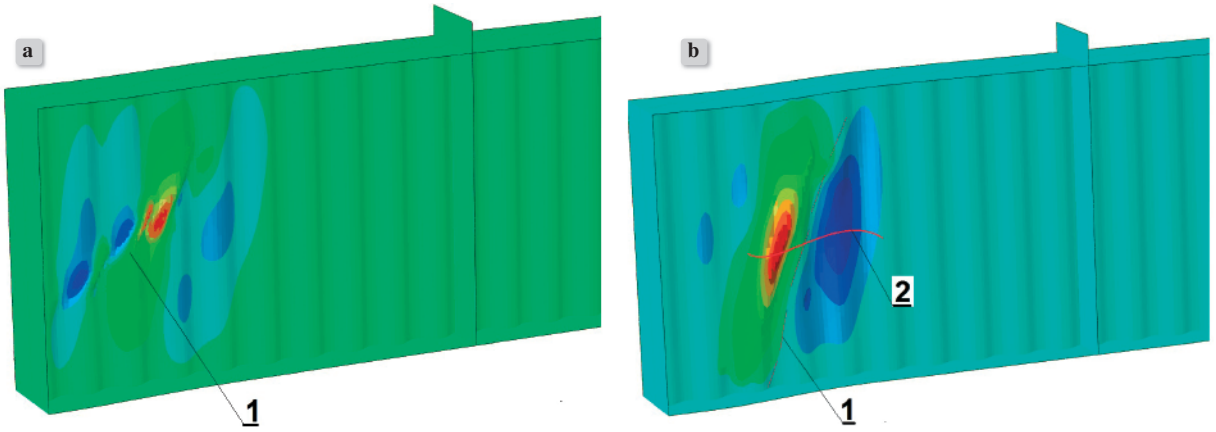

Figure 15.
Failure modes of numerical models: a) 1000x2 (stiffener 2x300x25); b) 1000x2.5 (stiffener 2x300x25)

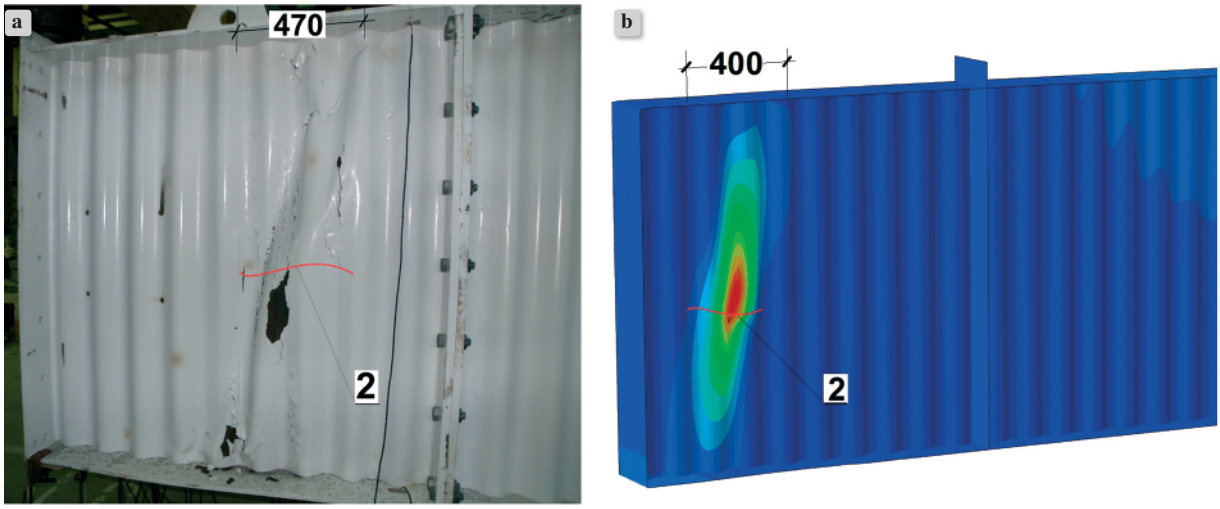

Figure 16.
Comparison of failure modes: a) experimental girder M 1.52 (1500x2: stiffener 2x300x25); b) numerical model 1500x2 (stiffener: 2x300x25)

that finished with the limit load reached at point $P_2(P_{uRd})$. It should be added that in experimental and numerical girders, a similar range of post-buckling resistance $P_1(P_{eB}) - P_2(P_{uRd})$ was found.

The FEM analysis confirmed that in cantilever SIN girders, a large range of elastic strain $0 - P_1(P_{eB})$ occurs, which produces an advantageous effect on the value of the first buckling load. The range is similar to that found in simply supported girders with rigid stiffeners at the girder ends.

Table 4 lists resistance of girders estimated with the FEM analysis. Column 4 gives limit load P_{uRd} measured with force P, whereas Column 5 shows first buckling load P_{eB} measured with force P. Column 6 lists load ratio P_{eB}/P_{uRd}.

4.4. Failrue modes in numerical models of cantilever girders

Figures 14, 15 and 16 show failure modes in numerical models of cantilever girders. Like it was the case with experimental girders, the web failure occurred suddenly in the cantilever part of the models. Support stiffeners remained undamaged.

For girders with the web height of $h_w = 500$ mm, failure modes obtained from experimental investigations and the FEM analysis turned out to be very much similar. In those girders, tension field led to the creation of the yield zone (1) (Fig. 11) related to the local instability of the web (L). In the final stage, flanges were loaded with unbalanced shear force, which resulted in their yield. Failure of cantilever girders with $h_w = 500$ mm corresponded to the failure mode of girders with the loading diagram of a simply supported beam.

In numerical models of cantilever girders with $h_w = 1000$ mm, two failure modes occurred. As regards numerical models with the web thickness of 2 mm, local mode of the web instability (L) was found (Fig. 15a). However, when the web thickness increased to 2.5 and 3 mm, failure mode was transformed to interactive instability mode (I) (Fig. 15b). The phenomenon indicates unambiguously that a change in the ratio $r/t_w/h_w$ (radius in the web roll-forming /web thickness /web height) is accompanied by a change in the geometric mode of the web instability from the local one to the interactive one.

In girders with the web height of $h_w = 1250$ and 1500 mm, tension field led to the creation of the yield zone and buckling of the web waves on the opposite side (2) (interactive instability – I). Further, that loaded flanges of girders (3) causing the yielding of flanges in the girder plane (Fig. 16 a and b). But at the same time, support stiffener restricted the action of the tension field forces which led to a reduction in the size of the web buckling area, and an increase in shear buckling resistance. Failure modes obtained from experimental investigations and the FEM analysis turned out to be congruent. The failure of cantilever girders with $h_w = 1250$ and 1500 mm was similar to the failure modes of girders with the loading diagram of a simply supported beam, ending with a rigid stiffener.

5. THE PROPOSED APPROACH FOR CANTILIVER GIRDERS OF CORRUGATED WEB

For cantilever girders, shear buckling resistance at the point of instability $P_1(P_{eB})$, estimated on the basis of experimental investigations and numerical analysis is:

$$\tau_{cr,B} = P_{eB} / h_w \, t_w \,, \tag{12}$$

where: P_{eB} – first buckling load; h_w, t_w – web height and thickness.

In cantilever girders of concern, similar to girders with the loading diagram of a simply supported beam, two modes of instability were found: local one and interactive one. Failure modes in cantilever girders indicate that the use of support stiffeners in cantilever girders produces an effect on the web failure mode similar to that brought about by rigid stiffeners in girders with the loading diagram of a simply supported beam. Stiffeners contribute to increase in shear buckling stress which leads to higher shear buckling resistance.

Thus, to estimate design shear buckling resistance τ_n, a computational model developed in study [15] was applied. The model relies on the estimation of interactive shear buckling resistance $\tau_{crI,6}$.

Interactive shear buckling resistance $\tau_{crI,6}$ [15] is:

$$\tau_{crI,6} = \frac{\tau_{cr,L} \cdot \tau_{cr,G}}{\left(\tau_{cr,L}^{\,6} + \tau_{cr,G}^{\,6}\right)^{\frac{1}{6}}} \,. \tag{13}$$

It was based on estimating local $\tau_{cr,L}$ and global $\tau_{cr,G}$ shear buckling stresses from classical equations (14), and also (15) [1]:

Table 5.
Comparison investigations, FEM analysis with design [6, 1] and proposed resistances (17)

Girder $h_w \times t_w$ [mm]	τ_{INV} [MPa]	τ_{FEM} [MPa]	$\frac{\tau_{INV}}{\tau_Y}$	$\frac{\tau_{FEM}}{\tau_Y}$	$\frac{\tau_{n,SB}}{\tau_Y}$	$\frac{\tau_{n,EC}}{\tau_Y}$	$\frac{\tau_{n,BA}}{\tau_Y}$	$\frac{\tau_{n,BA}}{\tau_{INV}}$	$\frac{\tau_{n,BA}}{\tau_{FEM}}$
1	2	3	4	5	6	7	8	9	10
500x2	147.0	149.1	0.80	0.92	0.79	0.86	0.86	1.09	0.93
500x2.5		149.4		0.92	0.79	0.91	0.86		0.93
500x3		149.7		0.92	0.79	0.95	0.86		0.93
1000x2	149.0	148.6	0.78	0.92	0.79	0.83	0.86	1.10	0.94
1000x2.5	152.0	148.5	0.90	0.92	0.79	0.88	0.86	0.96	0.94
1000x3	170.0	148.4	0.75	0.91	0.79	0.93	0.86	1.26	0.94
1250x2	121.6	144.0	0.86	0.89	0.79	0.82	0.85	1.01	0.96
1250x2.5		144.0		0.89	0.79	0.88	0.85		0.96
1250x3		143.9		0.89	0.79	0.92	0.86		0.96
1500x2	133.0	139.7	0.88	0.86	0.79	0.82	0.84	0.96	0.98
1500x2.5		141.8		0.87	0.79	0.87	0.85		0.97
1500x3		141.3		0.87	0.79	0.92	0.85		0.97
AVG.			**0.83**	**0.90**	**0.79**	**0.88**	**0.85**	**1.06**	**0.95**

$$\tau_{cr,L} = k_L \frac{\pi^2 E}{12\left(1-\upsilon^2\right)}\left[\frac{t_w}{s}\right]^2, \tag{14}$$

$$\tau_{cr,G} = k_G \frac{\left(D_y D_z^3\right)^{1/4}}{t_w h_w^2}\ . \tag{15}$$

In the solution adopted, the value of coefficient k_L at local instability was assumed as follows:

$$k_L = \left(5.34 + \frac{a_w^{0.5} \cdot s}{h_w t_w^{0.5}} + \frac{h_w}{a}\right), \tag{16}$$

where: s = 89 mm – length of the arc of half-sine wave, a_w = 40 mm – height of the two half-sine waves, a – span between stiffeners.

In addition, the value of coefficient k_G for global instability was assumed to be equal to 48.6. Hence the formula for estimating design shear buckling resistance in cantilever girders with corrugated web has the following form:

$$\tau_{n,BA} = \tau_y \left[\frac{2}{\lambda_{I,6}^{\ 6} + 5}\right]^{\frac{1}{6}}, \tag{17}$$

where: $\lambda_{I,6}$ – means interactive slenderness depending on the shear yield strength τ_y and the interactive shear buckling resistance $\tau_{crI,6}$:

$$\lambda_{I,6} = \sqrt{\frac{\tau_y}{\tau_{crI,6}}}\ . \tag{18}$$

In the case of girders where only a local instability takes place, the slenderness should be determined as dependent on the critical stresses at the local loss of stability $\tau_{cr,L}$. Design shear buckling resistance determined on the basis of formula (17) corresponds to shear buckling resistance obtained from experimental and numerical investigations as per Equation (12) in accordance with [12]. That means formula (17) is satisfied by all cantilever girders with corrugated web, the heights of which range from 500 to 1500 mm.

6. RESULTS AND ASSESSMENT OF THE ADOPTED SOLUTIONS

As for cantilever girders with corrugated web, they were girder cantilever parts that suffered failure. The value of design buckling resistance of cantilever girders was affected by the web failure mode. For the height of h_w = 500 mm, local (L) web instability developed. However, for girders with the height of h_w = 1000 – 1500 mm, the web failure resulted from interactive (I) shear instability.

Table 5 shows the results for design shear buckling resistance τ and normalized resistances τ/τ_y of cantilever girders. The comparison was made with respect to the results obtained from experimental investigations τ_{INV}, numerical analysis τ_{FEM}, proposal by Sause and Braxtan $\tau_{n,SB}$, EC3 $\tau_{n,EC}$ and the solution put forward by the author $\tau_{n,BA}$ (17).

The comparison of normalized buckling resistances as a function of slenderness obtained on the basis of experimental investigations (τ_{INV}/τ_y), numerical

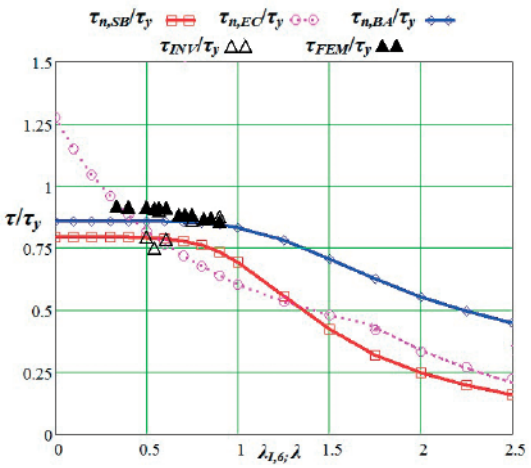

Figure 17.
Normalized shear resistance in function of the slenderness

analysis (τ_{FEM}/τ_y), proposal by Sause and Braxtan [6] ($\tau_{n,SB}/\tau_y$), EC 3 [1] ($\tau_{n,EC}/\tau_y$) and the one computed acc. the proposed solution ($\tau_{n,BA}/\tau_y$) was illustrated in Fig. 17. For Sause and Braxtan solution [6], the sinusoidal web wave was approximated using a trapezoidal shape of the fold.

Cantilever girders with corrugated web analysed in the study lose stability in the elastic-plastic range. The results of normalized shear resistance obtained from the FEM analysis (τ_{FE}/τ_y) are similar to the experimental results (τ_{INV}/τ_y).

The results of normalized resistance ($\tau_{n,SB}/\tau_y$) acc. the proposal by Sause and Braxtan [6] are slightly lower than those from the FEM analysis and the experiment. Additionally, in the elastic-plastic and plastic ranges at $\lambda < 0.6$, the commonly applied solution acc. EC3 produced normalized resistance results located in the range between the experimental ones and those based on the FEM analysis. EC3-based results, however, are more similar to FEM ones, and stress values are overestimated compared with the experiment.

Among all solutions analysed in the study that concern design shear buckling resistance, the solution put forward by the author gives the results that are closest to the experimental ones. The solution acc. equation (17) is based on the determination of interactive buckling resistance from equation (13). The solution of concern is also congruent with the FEM analysis results for high girders (h_w = 1000–1500 mm), in which interactive instability of the web occurs. The range of congruence between the adopted solution on the one hand, and the experiment and FEM analysis on the other is 0.95–1.06.

Similar to girders with the loading diagram of a simply supported beam, the experiment and FEM analysis show that cantilever SIN girders start losing stability below shear yield strength.

It should be noted that the formulas used for estimating interactive shear buckling resistance acc. equation (13) and design shear buckling resistance acc. equation (17) can be applied to the whole range of currently fabricated cantilever girders with support stiffener.

7. CONCLUSIONS

Cantilever girders with corrugated web are internally statically indeterminate systems. The failure of cantilever girders with corrugated web is related to the occurrence of tension line that affects the creation of the yield zone or the yield zone associated with the snap-through of the neighbouring waves of the web.

Shear buckling resistance depends on the web thickness and height. The resistance varies non-linearly with a change in the web height, due to local or interactive instability. Webs of cantilever girders with the height of h_w= 500 mm undergo local instability. In girders with the height of h_w = 1000 mm and higher, interactive instability is found.

Shear buckling resistance of the web in cantilever girders can be affected by the use of support stiffeners. They increase shear buckling resistance and the range of linear elastic displacements. The web shear buckling resistance with appropriate reserve constitutes a limit on the resistance of supports in SIN girders.

Additionally, increasing shear buckling resistance of supports in SIN girders with support stiffener reduces the need to utilise flat transition sheets that are applied for that purpose.

Behaviour of cantilever girders with corrugated web and support stiffener is similar to that of girders with the loading diagram of a simply supported beam, ending in a rigid stiffener.

Based on laboratory tests and the FEM analysis, a solution was proposed for estimating design shear buckling resistance of cantilever girders with corrugated web and support stiffener. The solution put forward (17) relies on the determination of interactive buckling resistance acc. equation (13). The rage of the adopted solution congruence with experimental results and FEM analysis is 0.95–1.06.

The solution accounts for the effect of the mutual correlation between local and global instability of the corrugated web in cantilever girders, and also for the beneficial influence of the support stiffener on shear buckling resistance. In addition, the solution provides a better representation of the design shear buckling resistance than it is the case with EC3-based approach [1], or that proposed by Sause and Braxtan [6], which respectively, overestimate or underestimate the results compared with the experimental findings.

It should be mentioned that in the tests on the supports of SIN girders, shear displacements of the cantilever ends were found to occur. They substantially exceed the displacements induced by bending. Significant scatter of shear displacements and global displacements of the support ends indicates that a need may arise to apply tension diagonal stiffeners acc. [26, 27].

ACKNOWLEDGEMENTS

The research is financed by National Science Centre based on grant no. No. N N506 072538.

REFERENCES

[1] EN 1993-1-5. 2008. Design of steel structures. Part 1-5: Plated structural elements.

[2] Driver RG, Abbas HH, Sause R. (2006). Shear behavior of corrugated web bridge girders. *Journal Structural Engineering*. *ASCE 132*(2), 195–203.

[3] Elgaaly M, Hamilton RW, Seshadri A. (1996) Shear strength of beams with corrugated webs. *Journal Structural Engineering, 122*(4), 390–398.

[4] Hamilton RW. Behavior of welded girder with corrugated webs. Ph.D. thesis. University of Maine; 1993.

[5] Sayed-Ahmed EY. (2001). Behavior of steel and (or) composite girders with corrugated steel webs. *Canadian Journal Civil Engineering, 28*(4), 656–672.

[6] Sause R, Braxtan TN. (2011). Shear strength of trapezoidal corrugated steel webs. *Journal of Constructional Steel Research*, 67, 223–236.

[7] Yi J, Gil H, Youm K, Lee H. (2008). Interactive shear buckling behavior of trapezoidally corrugated steel webs. *Engineering Structure*, *30*(6), 1659–1666.

[8] Abbas HH, Sause R, Driver RG. (2002). Shear strength and stability of high performance steel corrugated web girders. In: SSRC conference, 361–87.

[9] El-Metwally AS. (1998). Pre-stressed composite girders with corrugated steel webs. Thesis for degree of master, Calgary (Alberta, Canada): University of Calgary.

[10] Hassanein M.F, Kharoob O.F. (2013). Behavior of bridge girders with corrugated webs: (II) Shear strength and design. *Engineering Structures*, 57, 544–553.

[11] Hiroshi S., Hiroyuki I., Yohiaki I., Koichi K. (2003). Flexural shear behavior of composite bridge girder with corrugated steel webs around middle support. *JSCE*; 724(I-62), 49–67.

[12] Eldib MEA.-H. (2009). Shear buckling strength and design of curved corrugated steel webs for bridges. *Journal of Constructional Steel Research*, 65, 2129–2139.

[13] Kowal Z., Basiński W. (2013). Wpływ sztywności blach czołowych na postaciową wytrzymałość krytyczną dźwigarów o falistym środniku (The influence of the stiffness of end stiffeners on shear critical resistance of corrugated web of girders). *Konstrukcje Stalowe*, 3, 50–54. (in Polish)

[14] The research project N N506 072538 titled. (2013). Shaping frameworks girder on the corrugated web joined by end plates. Silesian University of Technology. (in Polish)

[15] Basiński W. (2018). Shear buckling of plate girders with corrugated web restrained by end stiffeners. *Periodica Polytechnica Civil Engineering. 62*(3), 757–771. https://doi.org/10.3311/PPci.11554.

[16] Profiles of corrugated web of SIN girders. Principles of dimensioning. Cracow University of Technology. Cracow 2002. (in Polish)

[17] Abaqus software adjustment to estimate resistance of corrugated web girders reinforced with end stiffeners. This research was supported in part by PL-GRID infrastructure, and also by the WIND grant.

[18] Moon J, Yi J, Choi BH, Lee H. (2009). Shear strength and design of trapezoidally corrugated steel webs. *Journal of Constructional Steel Research*, 65, 1198–205.

[19] Easley JT. (1975). Buckling formulas for corrugated metal shear diaphragms. *Journal Structural. Division*, SECF ST7, 1403–1417.

[20] Kowal Z., Basiński W. (2008). Wyznaczanie sztywności obrotowej doczołowych połączeń podatnych na podstawie pomiaru drgań dźwigarów (Determination of the rotational stiffness of semirigid end joints based on the measured vibrations). *Inżynieria i Budownictwo 64*(8), 457–461. (in Polish)

[21] Wuwer W., Zamorowski J., Swierczyna Sz. (2012). Lap joint stiffness according to Eurocode EC3 and experimental investigations results. *Archives of Civil and Mechanical Engineering, 12*(1), 95–104.

[22] Kuchta K. (2004). Resistance and stiffness of plate girders with corrugated web. Ph.D. thesis. Technical University of Cracow. (in Polish)

[23] EN 10002-1. 2001. Metallic materials – Tensile testing – Part 1: Method of test at ambient temperature.

[24] Basiński W., Kowal Z. (2018). Random strength parameters of steel corrugated webs and their influence on the resistance of SIN plate girders. *Architecture Civil Engineering, Environment*, *11*(3), 65–77. doi:10.21307/ACEE-2018-039.

[25] Memon B. A. (2004). Arc-length technique for nonlinear finite element analysis. *Journal of Zhejiang University SCIENCE, 5*(5), 618–628.

[26] Basiński W., Kowal Z. (2017). Investigations into the resistance of sin girders reinforced with tensioned diagonal braces. *Architecture Civil Engineering, Environment, 10*(1), 53–64.

[27] Basiński W., Kowal Z. (2017). FEM analysis of corrugated web girders reinforced with tensioned diagonal braces. *Architecture Civil Engineering Environment. 10*(1), 65–78.